Published in final edited form as:
Mol Pharm. 2011 December 5; 8(6): 2444–2453. doi:10.1021/mp200401p.

Hybrid peptide dendrimers for imaging of CXCR4 expression

Joeri Kuil[a], **Tessa Buckle**[a], **Joppe Oldenburg**[a], **Hushan Yuan**[b], **Lee Josephson**[b], and **Fijs W.B. van Leeuwen**[a,*]

[a]Division of Diagnostic Oncology, the Netherlands Cancer Institute Antoni van Leeuwenhoek Hospital, 1066 CX Amsterdam, The Netherlands [b]Center for Molecular Imaging Research, Massachusetts General Hospital and Harvard Medical School, Building 149, 13th Street, Charlestown, MA 02129, USA

Abstract

The chemokine receptor 4 (CXCR4), which is over-expressed in many types of cancer, is an emerging target in the field of molecular imaging and therapeutics. The CXCR4 binding of several peptides, including the cyclic Ac-TZ14011, has already been validated. In this study mono-, di- and tetrameric Ac-TZ14011-containing dendrimers were prepared and functionalized with a multimodality hybrid label, consisting of a Cy5.5-like flourophore and a DTPA chelate. Confocal microscopy revealed that all three dendrimers could target CXCR4 *in vitro*. The unlabeled dimer and tetramer had a slightly lower affinity for CXCR4 than the unlabeled monomer. However, when labeled with the multimodal label the CXCR4 affinity of the dimer and tetramer was significantly higher compared to the labeled monomer. On top of that, biodistribution studies revealed that the additional peptides in the dimer and tetramer reduced nonspecific tissue binding. Thus, multimerization of the cyclic Ac-TZ14011 peptide reduces the negative influence of the multimodal label on the receptor affinity and the biodistribution.

Keywords

CXCR4; peptides; dendrimers; multimodal hybrid imaging; fluorescence; SPECT/CT

Introduction

The chemokine receptor 4 (CXCR4) is a G-protein-coupled membrane receptor that is over-expressed in 23 types of cancer were it plays a role in, among others, the metastatic spread.[1–3] For this reason it is an emerging biomarker in the field of diagnostic oncology.[4] CXCR4 is also used as a target for cancer therapy and chemosensitization.[5–7] Several peptide antagonists for CXCR4 have been developed, including the potent 14 amino acid-containing disulfide-bridged Ac-TZ14011 cyclic peptide (Scheme 1).[8–11] The pharmacophore of this peptide consists of residues 2, 3, 5 and 14, and the peptide has only one free amine (D-Lys[8]), which is distant from the pharmacophore.[10–11] Several fluorescent dyes and indium-labeled DTPA have been used to label Ac-TZ14011 at D-Lys[8] and with these conjugates the CXCR4 binding has been validated *in vitro* and *in vivo*.[4,8–13] Recently we reported the first hybrid CXCR4 peptide, which consisted of Ac-TZ14011 and a multifunctional single attachment point (MSAP) label.[8] This MSAP label comprised a DTPA chelate, a CyAL-5.5$_b$ fluorophore and a reactive NHS ester.[14–16]

*Corresponding author. fw.v.leeuwen@nki.nl.

The development of multimodal probes is attaining a significant interest in the field of molecular imaging.[17–22] Such probes can be used in more than one imaging modality. Important imaging modalities are radionuclide-based imaging (SPECT and PET) and fluorescence-based optical imaging. Each modality has its own strengths and weaknesses, and therefore, a combination of modalities is often used in the clinic for optimal detection. Recently we have shown the added value of multimodal imaging agents in preclinical surgical guidance[8,23–24] and even in patients.[25] Multimodal probes can in principle also be used for postoperative pathology and assessment for the effectiveness of chemo- and/or immunotherapy.

Several receptor targeting peptides (e.g. RGD, octreotate, bombesin and Ac-TZ14011) have been functionalized with labels that combine radioactivity and fluorescence.[8,17] Such labels are often as large as the peptide used for the (tumor) specificity. Therefore, this hybrid labeling technology can have a significant (negative) influence on the receptor binding and the biodistribution. Especially the dye-driven, nonspecific uptake by organs and tissues is a substantial concern.[17] We reasoned in a recent review that multimeric peptide dendrimers, consisting of multiple peptides (e.g. 4) and one hybrid label, could reduce the influence of the label.[17] Multimerization is well known to enhance the receptor affinity and specificity.[26–31] Furthermore, multimerization increases the amount of peptides with respect to the label, which may shield the label from the biological environment.[17]

The strategy of peptide multimerization has already been successfully applied with radiolabels and fluorescent labels.[32–36] However, only nano-sized multimeric peptides have been prepared with both a radiolabel and a fluorescent label.[37–38] These “large” nanoparticles suffered from high nonspecific (liver) uptake and were not able to extravasate from blood vessels into the tumor.[37–38] Surprisingly, small hybrid peptide dendrimers, which have generally a better biodistribution, have never been reported. Here, we report the first hybrid Ac-TZ14011-containing dimeric and tetrameric dendrimers. These dendrimers are based on our previously reported multimodal Ac-TZ14011-MSAP peptide (**3**) (Scheme 1).[8]

Results and Discussion

Design and synthesis

The main aim of our chemical design was to minimize the negative influence of the multimodal MSAP label on receptor binding and tumor targeting observed for the previously reported monomer Ac-TZ14011-MSAP (**3**).[8] To achieve this, we prepared dimeric and tetrameric dendrimers, where the MSAP label is placed in the core of the dendrimer (Figure 1). The dendrimers were based on glutamic acid and additional β-alanine spacers were incorporated to ensure that the peptide epitopes would not hinder the CXCR4 binding of the other peptides. This was verified by inserting the models of Figure 1 into the crystal structure of CXCR4.[39] In the models of CXCR4 binding the spacers appear to be long enough (see Figure S1). The relative short spacers enable the peptides to shield the MSAP label from the biological environment to some extend (Figure 1). As a consequence of the short spacers, the dendrimers will most likely not be able the bind multiple CXCR4 receptors simultaneously, because large spacers of 5.5 – 6.5 nm are required to achieve this.[40] However, our design can in principle also result in higher binding affinities due to an effect named statistical rebinding.[26–27] This effect is caused by an overall slower off-rate of the multimeric compound due to the close proximity of other peptide epitopes, which can replace the bound peptide when released form the binding site of CXCR4.

The synthesis of the dendrimers is outlined in Scheme 1. First Boc-Glu(β-Ala-OH)-β-Ala-OH (**4**) was prepared, after which it was functionalized with Ac-TZ14011 (**2**), yielding the

Boc-protected dimer $(Ac\text{-}TZ14011)_2$ (**5**) (Scheme 1). The Boc group was removed with TFA and the MSAP reagent (**1**) was attached to the free amine in the core of the molecule yielding multimodal compound **7**. Alternatively, an excess of dimeric derivative **5** were reacted with Boc-Glu(β-Ala-OH)-β-Ala-OH (**4**) to obtain the Boc-protected tetrameric peptide dendrimer **8**. Boc deprotection and subsequently conjugation with **1** yielded the tetrameric MSAP derivative **10**.

In vitro evaluation

Previously we have demonstrated that monomer Ac-TZ14011-MSAP (**3**) was able to discriminate between MDAMB231 cells, which express basal levels of CXCR4, and $MDAMB231^{CXCR4+}$ cells, which over-express CXCR4 in fourfold.[8] Furthermore, the binding affinity of Ac-TZ14011 (**2**) and Ac-TZ14011-MSAP (**3**) for CXCR4 has been established.[8] For comparison of the Ac-TZ14011-based dendrimers, the binding affinity is the most reliable point of comparison. Therefore, the binding affinity of dimers **6** and **7** and tetramers **9** and **10** were compared to the monomers **2** and **3** using the $MDAMB231^{CXCR4+}$ cells.

The CXCR4 receptor affinity of the unlabeled constructs was determined using a previously reported cell-based competition assay, where the unlabeled peptides compete with monomer Ac-TZ14011-MSAP (**3**) for CXCR4 binding (Figure 2A).[8] The dissociation constant (K_D) of the monomer Ac-TZ14011 (**2**) has previously been reported to be 8.61 nM (Table 1).[8] The receptor affinity of both dimer $(Ac\text{-}TZ14011)_2$ (**6**) and tetramer $(Ac\text{-}TZ14011)_4$ (**9**) was found to be slightly lower; 23.5 nM and 30.6 nM, respectively. Thus, the presence of the additional peptides does not substantially hinder the binding to CXCR4. On the other hand, a multivalency effect based on e.g. bivalent binding or statistical rebinding was not observed. Our previously reported iridium complexes outfitted with one, two or three Ac-TZ14011 peptides also did not display a considerable multivalency effect.[9] These findings are not uncommon for peptides binding to G-protein coupled receptors (GPCRs), as multimeric octreotides also do not bind in a multivalent manner to the somatostatin GPCR.[41–42] It is apparently very challenging to design spacers that can position the binding epitopes correctly for simultaneous binding to multiple GPCRs.

Also the receptor affinity of the MSAP-labeled constructs **3**, **7** and **10** was determined using a saturation binding experiment (Figure 2B). The affinity of the monomer Ac-TZ14011-MSAP (**3**) was previously reported by us and amounts 186.9 nM (Table 1).[8] Interestingly, the dimer $(Ac\text{-}TZ14011)_2$-MSAP (**7**) had a twofold higher affinity; namely 93.1 nM. This in contrast with the trend found for the unlabeled peptide derivatives: the unlabeled dimer $(Ac\text{-}TZ14011)_2$ (**6**) has a lower CXCR4 affinity than the monomer Ac-TZ14011 (**2**) (Table 1). Apparently the additional peptide moiety reduces the negative influence of the MSAP label on the receptor affinity. For the tetramer $(Ac\text{-}TZ14011)_4$-MSAP (**10**) the same trend was observed (K_D = 80.5 nM), although the improvement with respect to dimer $(Ac\text{-}TZ14011)_2$-MSAP (**7**) was minimal. The saturation binding curve showed that the nonspecific cell binding was considerably reduced for the tetramer $(Ac\text{-}TZ14011)_4$-MSAP (**10**), i.e. the linear part of the curve is considerable less steep than that of the monomer Ac-TZ14011-MSAP (**3**) (Figure 2B).

Next to the CXCR4 affinity, also the cellular distribution of the MSAP-labeled compounds **3**, **7** and **10** was evaluated using confocal microscopy. $MDAMB231^{CXCR4+}$ cells were incubated with 1 μM of compound for 1 hour at 4 °C, to minimize active internalization. All three peptide conjugates displayed cell membrane staining (Figure 3) which is in accordance with the location of the CXCR4 receptor.[8–11] Also a small amount of internalization of compounds **3**, **7** and **10** was observed, most likely caused by the fact that the confocal

imaging was performed at 37 °C, resulting in receptor mediated endocytosis. As a negative control, cells were incubated with the MSAP label (**1**) alone, of which the active NHS ester was hydrolyzed prior incubation. The MSAP label showed almost no staining (Figure 3D), and therefore, the cell membrane staining pattern of compounds **3**, **7** and **10** is driven by the targeting peptide moieties and is not caused by nonspecific cell membrane binding of the MSAP label.

The effect of the monomers **2** and **3**, dimers **6** and **7** and tetramers **9** and **10** on the cell viability was determined to exclude any artifacts (Figure 2C–D). None of the six compounds had an influence on the cell viability up to concentrations of 1 μM. At 10 μM monomer Ac-TZ14011 (**2**) and dimer $(Ac\text{-}TZ14011)_2$ (**6**) still did not show significant toxicity, whereas tetramer $(Ac\text{-}TZ14011)_4$ (**9**) substantially reduced the cell viability (Figure 2C). The trend that the increasing multimeric character of the Ac-TZ14011 peptide leads to more cytotoxicity has previously been observed by us.[9] We reasoned that the considerable amount of positive charges in the multimeric Ac-TZ14011 constructs is most likely the cause of decreasing cell viability.[9]

Based on the *in vitro* experiments the dimer $(Ac\text{-}TZ14011)_2$-MSAP (**7**) seems to be the most promising imaging probe. It has the practically the same high affinity for CXCR4 as the tetramer $(Ac\text{-}TZ14011)_4$-MSAP (**10**), has considerable less influence on the cell viability and is easier to prepare.

In vivo evaluation

In vivo imaging studies were performed to evaluate the tumor targeting of the MSAP peptides **3**, **7** and **10**. Therefore, mice with CXCR4 positive "spontaneous" MIN-O tumors were used instead of the $MDAMB231^{CXCR4+}$ cell line, because the CXCR4 expression in non-transfected $MDAMB231^{CXCR4+}$ cells decreases to basal levels *in vivo*. Mice were injected with ^{111}In-labeled compounds **3**, **7** and **10**, and after 24 h the mice were imaged with SPECT/CT imaging (Figure 4).

After imaging the mice were sacrificed and biodistribution studies were conducted (Table 2). As a reference also the biodistribution of the peptide with only a DTPA chelate as an imaging label, Ac-TZ14011-DTPA (**11**), is given (see Supporting Information for the structure). As a negative control, the MSAP label (**1**) was used without further functionalization (reactive group was neutralized) in non-tumor bearing mice. The hybrid label displayed enhanced blood, heart, muscle, stomach and intestinal uptake, which suggests that the MSAP label is cleared slower than Ac-TZ14011-DTPA (**11**). This is most likely caused by the hydrophobic character of the $CyAL\text{-}5.5_b$ fluorophore. The MSAP label had a reduced kidney uptake compared to Ac-TZ14011-DTPA (**11**).

The monomer Ac-TZ14011-MSAP (**3**) gave increased liver and intestinal uptake and reduced kidney uptake compared to the reference Ac-TZ14011-DTPA (**11**), suggesting a changing in the clearance route (Table 2). The monomer Ac-TZ14011-MSAP (**3**) displayed a more than five times higher tumor uptake than Ac-TZ14011-DTPA (**11**). However, this increase was accompanied with higher nonspecific uptake in the lungs, heart, spleen, stomach, intestines and muscles, most likely caused by nonspecific binding of the relative hydrophobic $CyAL\text{-}5.5_b$ fluorophore. This resulted in a lower tumor-to-muscle ratio compared to Ac-TZ14011-DTPA (**11**) (4.55 and 6.67, respectively) (Table 3). As mentioned in the introduction, a higher nonspecific binding and lower tumor-to-muscle ratio is common for monomeric multimodal peptides.[17] The reason for this is the relative large size of the hybrid imaging label.

The dimer $(Ac\text{-}TZ14011)_2$-MSAP (**7**) had a similar uptake profile as monomer Ac-TZ14011-MSAP (**3**) (Table 2). However, the muscle uptake was significantly lower than that of the monomeric MSAP peptide ($P < 0.001$; all significant differences with respect to compound **3** are denoted in Table S1). Thus, the enhanced nonspecific muscle uptake of monomer Ac-TZ14011-MSAP (**3**) compared to Ac-TZ14011-DTPA (**11**) is largely eliminated by the additional peptide in compound **7**. Also the tumor and heart uptake was lower, although this was not significant. The decrease of the uptake in the muscle and heart was larger than in the tumor, resulting in an improved tumor-to-muscle ratio (Table 3). This improvement was not significant, because the standard deviation of dimer $(Ac\text{-}TZ14011)_2$-MSAP (**7**) was rather high.

The tetramer $(Ac\text{-}TZ14011)_4$-MSAP (**10**) continued the trend of the mono- and dimer (Table 2). The uptake in the tumor and in the heart was again slightly lower than that of dimer $(Ac\text{-}TZ14011)_2$-MSAP (**7**). Because the uptake in the muscle was already very low for dimer $(Ac\text{-}TZ14011)_2$-MSAP (**7**), this was not reduced further for tetramer $(Ac\text{-}TZ14011)_4$-MSAP (**10**). As a consequence, the tumor-to-muscle ratio of the tetramer was somewhat lower compared to the dimer (**7**) (Table 3). However, nonspecific uptake of tetramer $(Ac\text{-}TZ14011)_4$-MSAP (**10**) in organs such as the lungs, heart and liver was again slightly lower compared to dimer $(Ac\text{-}TZ14011)_2$-MSAP (**7**). Thus, the two additional peptides seem to have decreased the MSAP driven nonspecific uptake even further.

The results of the *in vivo* studies show that the additional peptide in the dimer reduced the negative influence of the multimodal MSAP label, yielding a tumor-to-muscle ratio higher than that of Ac-TZ14011-DTPA (**11**). The addition of two more peptides, as in tetramer $(Ac\text{-}TZ14011)_4$-MSAP (**10**), did not result in a further improvement of the tumor-to-muscle ratio.

Conclusions

Multimerization resulted in both the dimer and tetramer in reduction of the nonspecific binding caused by the multimodal label. The CXCR4 affinity of dimer $(Ac\text{-}TZ14011)_2$-MSAP (**7**) and tetramer $(Ac\text{-}TZ14011)_4$-MSAP (**10**) is comparable, the dimer has less influence on the cell viability and the tumor-to-muscle ratio of the dimer is higher. Thus, dimer $(Ac\text{-}TZ14011)_2$-MSAP (**7**) is the most promising CXCR4 imaging probe.

This concept of multimerization of multimodal peptides can also be applied to other targeting peptides such as RGD. It seems that the use highly positively charged peptides and highly hydrophobic peptides should be avoided to suppress the cytotoxicity and the nonspecific cell and tissue binding. In this manner our concept could result in even more promising imaging agents.

Supplementary Material

Refer to Web version on PubMed Central for supplementary material.

Acknowledgments

This research is supported, in part, by a KWF-translational research award (Grant No. PGF 2009-4344; FvL), and within the framework of CTMM, the Centre for Translational Molecular Medicine (http://www.ctmm.nl), project Breast CARE (grant 030-104; JK).

References

1. Teicher BA, Fricker SP. CXCL12 (SDF-1)/CXCR4 pathway in cancer. Clin. Cancer Res. 2010; 16:2927–2931. [PubMed: 20484021]
2. Kulbe H, Levinson NR, Balkwill F, Wilson JL. The chemokine network in cancer-much more than directing cell movement. Int. J Dev. Biol. 2004; 48:489–496. [PubMed: 15349823]
3. Furusato B, Mohamed A, Uhlen M, Rhim JS. CXCR4 and cancer. Pathol. Int. 2010; 60:497–505. [PubMed: 20594270]
4. Nimmagadda S, Pullambhatla M, Stone K, Green G, Bhujwalla ZM, Pomper MG. Molecular imaging of CXCR4 receptor expression in human cancer xenografts with [^{64}Cu]AMD3100 positron emission tomography. Cancer Res. 2010; 70:3935–3944. [PubMed: 20460522]
5. Hassan S, Buchanan M, Jahan K, Aguilar-Mahecha A, Gaboury L, Muller WJ, Alsawafi Y, Mourskaia AA, Siegel PM, Salvucci O, Basik M. CXCR4 peptide antagonist inhibits primary breast tumor growth, metastasis and enhances the efficacy of anti-VEGF treatment or docetaxel in a transgenic mouse model. Int. J. Cancer. 2011; 129:225–232. [PubMed: 20830712]
6. Azab AK, Runnels JM, Pitsillides C, Moreau AS, Azab F, Leleu X, Jia X, Wright R, Ospina B, Carlson AL, Alt C, Burwick N, Roccaro AM, Ngo HT, Farag M, Melhem MR, Sacco A, Munshi NC, Hideshima T, Rollins BJ, Anderson KC, Kung AL, Lin CP, Ghobrial IM. CXCR4 inhibitor AMD3100 disrupts the interaction of multiple myeloma cells with the bone marrow microenvironment and enhances their sensitivity to therapy. Blood. 2009; 113:4341–4351. [PubMed: 19139079]
7. Nervi B, Ramirez P, Rettig MP, Uy GL, Holt MS, Ritchey JK, Prior JL, Piwnica-Worms D, Bridger G, Ley TJ, DiPersio JF. Chemosensitization of acute myeloid leukemia (AML) following mobilization by the CXCR4 antagonist AMD3100. Blood. 2009; 113:6206–6214. [PubMed: 19050309]
8. Kuil J, Buckle T, Yuan H, Van den Berg NS, Oishi S, Fujii N, Josephson L, Van Leeuwen FWB. Synthesis and evaluation of a bimodal CXCR4 antagonistic peptide. Bioconjugate Chem. 2011; 22:859–864.
9. Kuil J, Steunenberg P, Chin PTK, Oldenburg J, Jalink K, Velders AH, Van Leeuwen FWB. Peptide-functionalized luminescent iridium complexes for lifetime imaging of CXCR4 expression. ChemBioChem. 2011
10. Nomura W, Tanabe Y, Tsutsumi H, Tanaka T, Ohba K, Yamamoto N, Tamamura H. Fluorophore labeling enables imaging and evaluation of specific CXCR4-ligand interaction at the cell membrane for fluorescence-based screening. Bioconjugate Chem. 2008; 19:1917–1920.
11. Oishi S, Masuda R, Evans B, Ueda S, Goto Y, Ohno H, Hirasawa A, Tsujimoto G, Wang Z, Peiper SC, Naito T, Kodama E, Matsuoka M, Fujii N. Synthesis and application of fluorescein- and biotin-labeled molecular probes for the chemokine receptor CXCR4. ChemBioChem. 2008; 9:1154–1158. [PubMed: 18412193]
12. Hanaoka H, Mukai T, Tamamura H, Mori T, Ishino S, Ogawa K, Iida Y, Doi R, Fujii N, Saji H. Development of a ^{111}In-labeled peptide derivative targeting a chemokine receptor, CXCR4, for imaging tumors. Nucl. Med. Biol. 2006; 33:489–494. [PubMed: 16720240]
13. Van den Berg NS, Buckle T, Kuil J, Wesseling J, Van Leeuwen FWB. Direct fluorescent detection of CXCR4 using a targeted peptide antagonist. accepted in Trans. Oncol. 2010
14. Garanger E, Aikawa E, Reynolds F, Weissleder R, Josephson L. Simplified syntheses of complex multifunctional nanomaterials. Chem. Commun. 2008:4792–4794.
15. Shao F, Yuan H, Josephson L, Weissleder R, Hilderbrand SA. Facile synthesis of monofunctional pentamethine carbocyanine fluorophores. Dyes Pigments. 2011; 90:119–122.
16. Garanger E, Blois J, Hilderbrand SA, Shao F, Josephson L. Divergent oriented synthesis for the design of reagents for protein conjugation. J. Comb. Chem. 2010; 12:57–64. [PubMed: 19928910]
17. Kuil J, Velders AH, Van Leeuwen FWB. Multimodal tumor-targeting peptides functionalized with both a radio-and a fluorescent-label. Bioconjugate Chem. 2010; 21:1709–1719.
18. Louie A. Multimodality imaging probes: design and challenges. Chem. Rev. 2010; 110:3146–3195. [PubMed: 20225900]

19. Thorp-Greenwood FL, Coogan MP. Multimodal radio- (PET/SPECT) and fluorescence imaging agents based on metallo-radioisotopes: current applications and prospects for development of new agents. Dalton Trans. 2011; 40:6129–6143. [PubMed: 21225080]
20. Culver J, Akers W, Achilefu S. Multimodality molecular imaging with combined optical and SPECT/PET modalities. J. Nucl. Med. 2008; 49:169–172. [PubMed: 18199608]
21. Lee S, Chen X. Dual-modality probes for in vivo molecular imaging. Mol. Imaging. 2009; 8:87–100. [PubMed: 19397854]
22. Buckle T, Chin PTK, van Leeuwen FWB. (Non-targeted) radioactive/fluorescent nanoparticles and their potential in combined pre- and intraoperative imaging during sentinel lymph node resection. Nanotechnology. 2010; 21:482001. [PubMed: 21063057]
23. Buckle T, van Leeuwen AC, Chin PTK, Janssen H, Muller SH, Jonkers J, van Leeuwen FWB. A self-assembled multimodal complex for combined pre- and intraoperative imaging of the sentinel lymph node. Nanotechnology. 2010; 21:355101. [PubMed: 20689167]
24. Buckle T, Chin PTK, van den Berg NS, Loo CE, Koops W, Gilhuijs KG, van Leeuwen FWB. Tumor bracketing and safety margin estimation using multimodal marker seeds: a proof of concept. J. Biomed. Opt. 2010; 15:056021. [PubMed: 21054115]
25. Van der Poel HG, Buckle T, Brouwer OR, Valdés Olmos RA, Van Leeuwen FWB. Intraoperative laparoscopic fluorescence guidance to the sentinel lymph node in prostate cancer patients; clinical proof of concept of an integrated functional imaging approach using a multimodal tracer. Eur. Urol. 2011
26. Kiessling LL, Gestwicki JE, Strong LE. Synthetic multivalent ligands as probes of signal transduction. Angew. Chem. Int. Ed. 2006; 45:2348–2368.
27. Pieters RJ. Maximising multivalency effects in protein-carbohydrate interactions. Org. Biomol. Chem. 2009; 7:2013–2025. [PubMed: 19421435]
28. Mammen M, Choi SK, Whitesides GM. Polyvalent interactions in biological systems: implications for design and use of multivalent ligands and inhibitors. Angew. Chem. Int. Ed. 1998; 37:2754–2794.
29. Lundquist JJ, Toone EJ. The cluster glycoside effect. Chem. Rev. 2002; 102:555–578. [PubMed: 11841254]
30. Kitov PI, Bundle DR. On the nature of the multivalency effect: a thermodynamic model. J. Am. Chem. Soc. 2003; 125:16271–16284. [PubMed: 14692768]
31. Reczek JJ, Kennedy AA, Halbert BT, Urbach AR. Multivalent recognition of peptides by modular self-assembled receptors. J. Am. Chem. Soc. 2009; 131:2408–2415. [PubMed: 19199617]
32. Cheng Z, Wu Y, Xiong Z, Gambhir SS, Chen X. Near-infrared fluorescent RGD peptides for optical imaging of integrin $\alpha_v\beta_3$ expression in living mice. Bioconjugate Chem. 2005; 16:1433–1441.
33. Liu S. Radiolabeled cyclic RGD peptides as integrin $\alpha_v\beta_3$-targeted radiotracers: maximizing binding affinity via bivalency. Bioconjugate Chem. 2009; 20:2199–2213.
34. Almutairi A, Rossin R, Shokeen M, Hagooly A, Ananth A, Capoccia B, Guillaudeu S, Abendschein D, Anderson CJ, Welch MJ, Frechet JM. Biodegradable dendritic positron-emitting nanoprobes for the noninvasive imaging of angiogenesis. Proc. Natl. Acad. Sci. U.S.A. 2009; 106:685–690. [PubMed: 19129498]
35. Galibert M, Sancey L, Renaudet O, Coll JL, Dumy P, Boturyn D. Application of click-click chemistry to the synthesis of new multivalent RGD conjugates. Org. Biomol. Chem. 2010; 8:5133–5138. [PubMed: 20835451]
36. Abiraj K, Jaccard H, Kretzschmar M, Helm L, Maecke HR. Novel DOTA-based prochelator for divalent peptide vectorization: synthesis of dimeric bombesin analogues for multimodality tumor imaging and therapy. Chem. Commun. 2008:3248–3250.
37. Cai W, Chen K, Li ZB, Gambhir SS, Chen X. Dual-function probe for PET and near-infrared fluorescence imaging of tumor vasculature. J. Nucl. Med. 2007; 48:1862–1870. [PubMed: 17942800]
38. Boswell CA, Eck PK, Regino CA, Bernardo M, Wong KJ, Milenic DE, Choyke PL, Brechbiel MW. Synthesis, characterization, and biological evaluation of integrin alphavbeta3-targeted PAMAM dendrimers. Mol. Pharm. 2008; 5:527–539. [PubMed: 18537262]

39. Wu B, Chien EYT, Mol CD, Fenalti G, Liu W, Katritch V, Abagyan R, Brooun A, Wells P, Bi FC, Hamel DJ, Kuhn P, Handel TM, Cherezov V, Stevens RC. Structures of the CXCR4 chemokine GPCR with smallmolecule and cyclic peptide antagonists. Science. 2010; 330:1066–1071. [PubMed: 20929726]

40. Tanaka T, Nomura W, Narumi T, Masuda A, Tamamura H. Bivalent ligands of CXCR4 with rigid linkers for elucidation of the dimerization state in cells. J. Am. Chem. Soc. 2010; 132:15899–15901. [PubMed: 20973474]

41. Yim CB, Boerman OC, de Visser M, de Jong M, Dechesne AC, Rijkers DTS, Liskamp RMJ. Versatile conjugation of octreotide to dendrimers by cycloaddition ("click") chemistry to yield high-affinity multivalent cyclic peptide dendrimers. Bioconjugate Chem. 2009; 20:1323–1331.

42. Yim CB, Dijkgraaf I, Merkx R, Versluis C, Eek A, Mulder GE, Rijkers DTS, Boerman OC, Liskamp RMJ. Synthesis of DOTA-conjugated multimeric [Tyr^3]octreotide peptides via a combination of Cu(I)-catalyzed "click" cycloaddition and thio acid/sulfonyl azide "sulfo-click" amidation and their in vivo evaluation. J. Med. Chem. 2010; 53:3944–3953. [PubMed: 20411957]

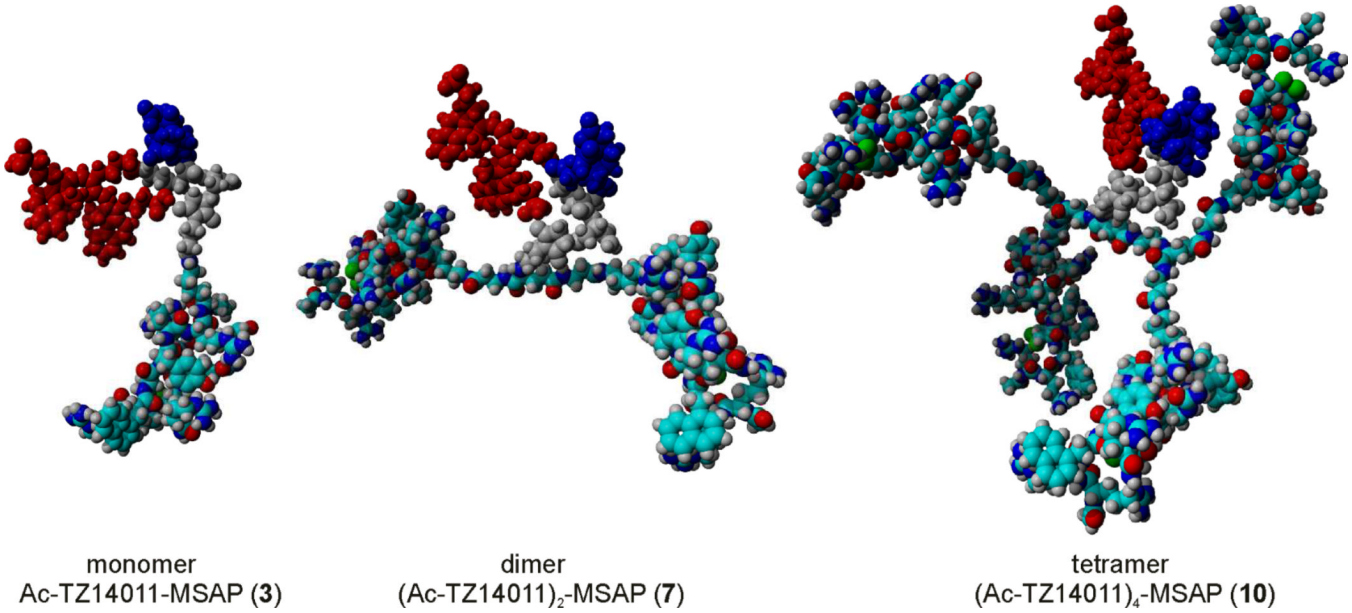

Figure 1.

Molecular models of the mono-, di- and tetrameric Ac-TZ14011 dendrimers with the MSAP label. For clarity, the MSAP label is not colored by element: the CyAL-5.5$_b$ fluorophore is displayed in red, the indium-bound DTPA chelate in blue and the spacer in grey. In the dimer and, especially, in the tetramer a smaller percentage of the whole molecule comprises the MSAP label.

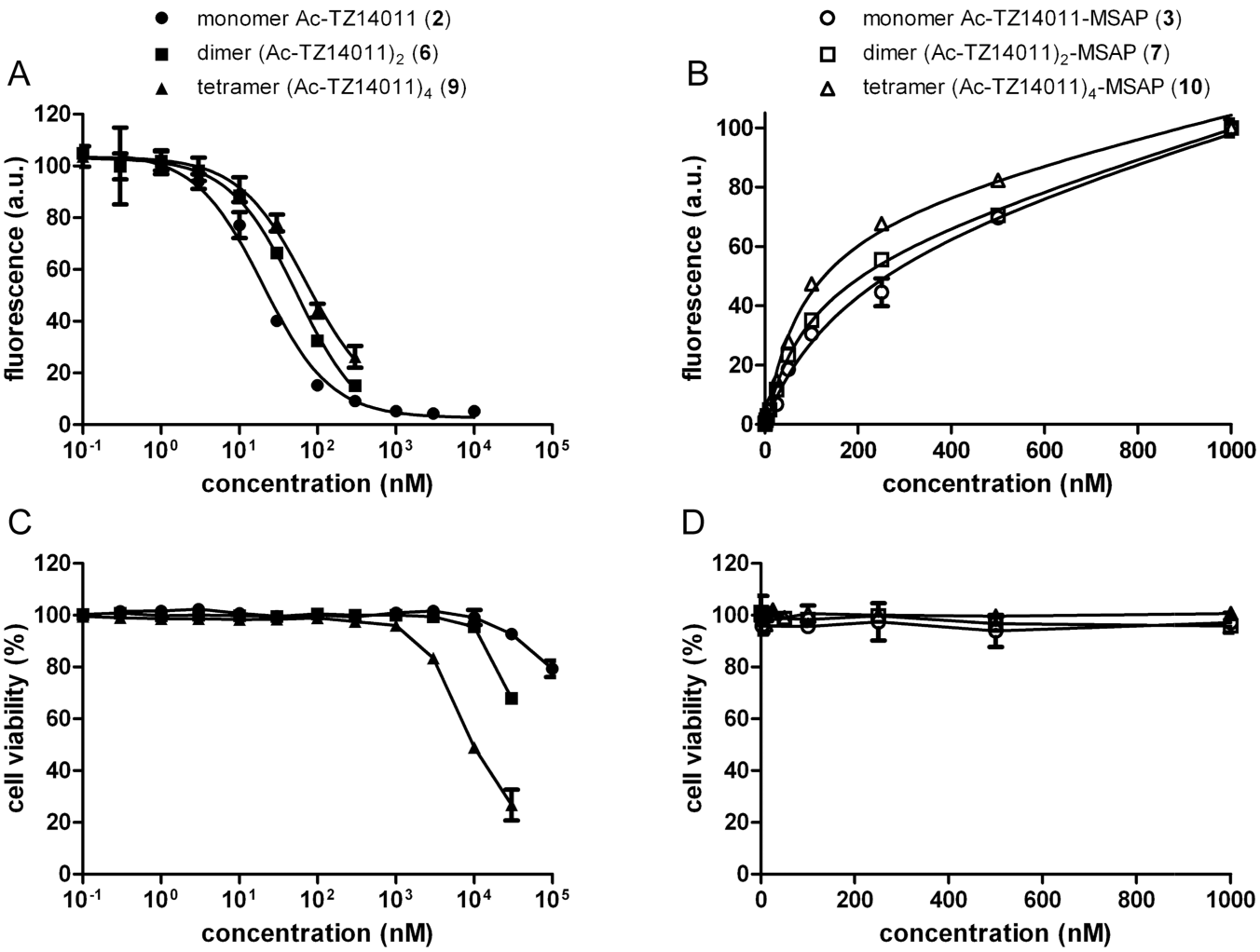

Figure 2.

A) Competition experiments of the compounds **2**, **6** and **9** in the presence of 250 nM of Ac-TZ14011-MSAP (**3**). B) Saturation binding experiments of compounds **3**, **7** and **10**. C and D) Cell viability of MDAMB231^{CXCR4+} cells in the presence of different concentrations compounds **2**, **6** and **9** (C) and compounds **3**, **7** and **10** (D). For all graphs the bars represent average ± SD.

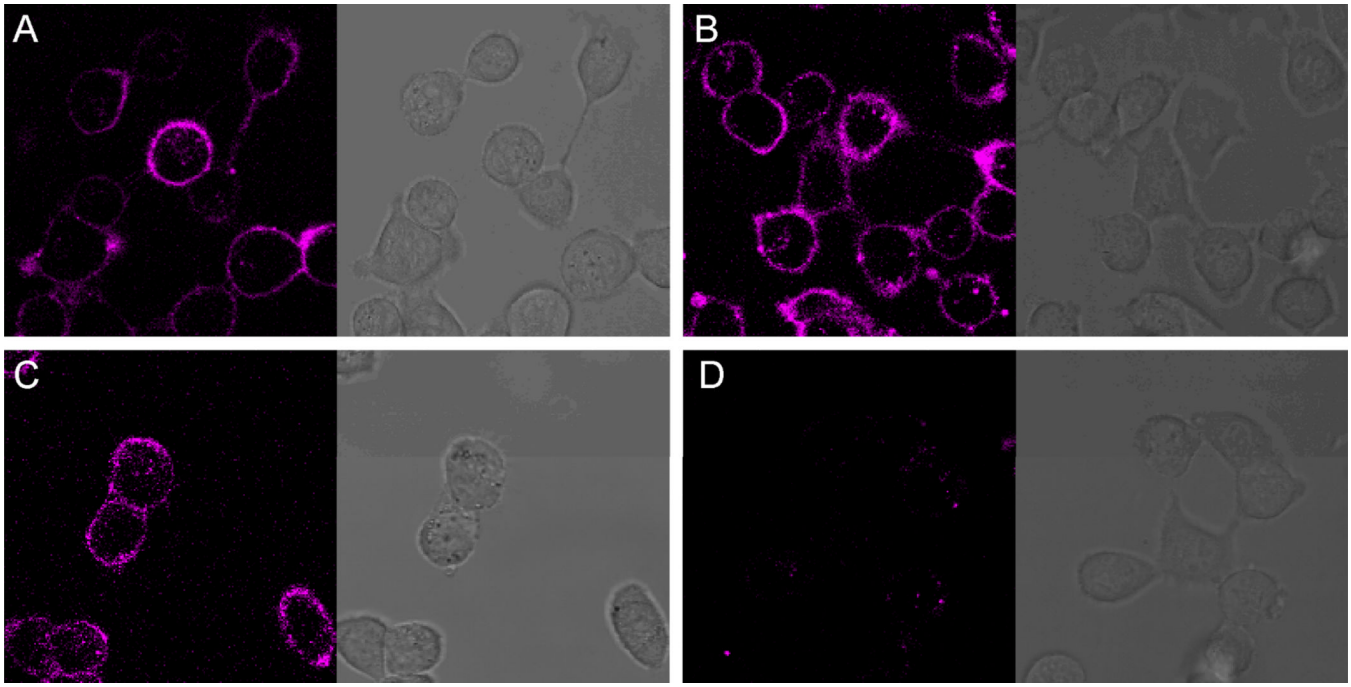

Figure 3.

Confocal microscopy and transmission images of the multimodal peptide conjugates on MDAMB231^{CXCR4+} cells. A) 1 μM of monomer Ac-TZ14011-MSAP (**3**); B) 1 μM of dimer $(Ac\text{-}TZ14011)_2$-MSAP (**6**); C) 1 μM of tetramer $(Ac\text{-}TZ14011)_4$-MSAP (**10**); D) 1 μM of MSAP (**1**).

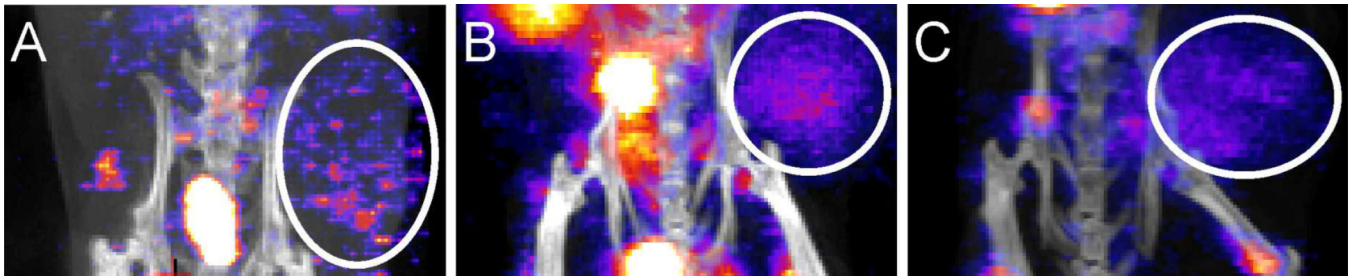

Figure 4.
SPECT/CT and fluorecence imaging. SPECT/CT of A) monomer Ac-TZ14011-MSAP (**3**), B) dimer $(Ac\text{-}TZ14011)_2$-MSAP (**7**) and C) tetramer $(Ac\text{-}TZ14011)_4$-MSAP (**10**).

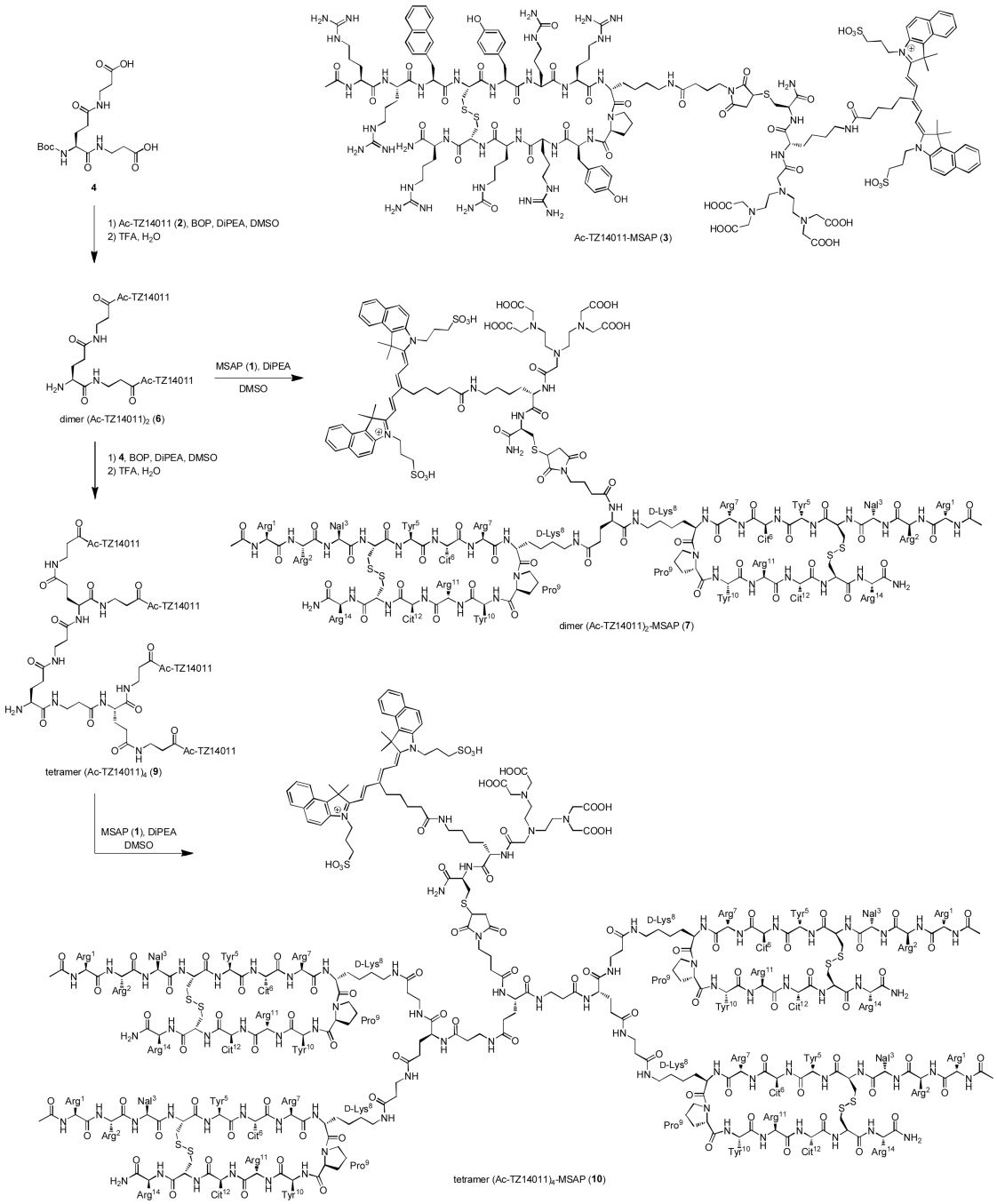

Scheme 1.

Synthesis of dimer (Ac-TZ14011)$_2$ (**6**), dimer (Ac-TZ14011)$_2$-MSAP (**7**), tetramer (Ac-TZ14011)$_4$ (**9**) and tetramer (Ac-TZ14011)$_4$-MSAP (**10**) and the structure of monomer Ac-TZ14011-MSAP (**3**).

Table 1

Dissociation constants (K_D) of the Ac-TZ14011 derivatives.

compound	K_D (nM)	
	unlabeled	MSAP-labeled
monomers **2** and **3**	8.61 ± 1.42	186.9 ± 52.4
dimers **6** and **7**	23.5 ± 2.43	93.1 ± 10.1
tetramers **9** and **10**	30.6 ± 4.84	80.5 ± 11.6

Table 2

Biodistribution of ^{111}In-labeled Ac-TZ14011-DTPA (**11**), monomer Ac-TZ14011-MSAP (**3**), dimer (Ac-TZ14011)$_2$-MSAP (**7**), tetramer (Ac-TZ14011)$_4$-MSAP (**10**) and MSAP label (**1**) in MIN-O tumor bearing mice at 24 h post injecting.

	uptake (%ID/g)				
tissue	**Ac-TZ14011-DTPA (11)**	**MSAP label (1)**	**monomer Ac-TZ14011-MSAP (3)**	**dimer (Ac-TZ14011)$_2$-MSAP (7)**	**tetramer (Ac-TZ14011)$_4$-MSAP (10)**
Blood	0.01 ± 0.00	0.32 ± 0.09 **	0.14 ± 0.02 ***	0.14 ± 0.03 **	0.11 ± 0.01 ***
Brain	0.00 ± 0.00	0.03 ± 0.01	0.02 ± 0.00	0.03 ± 0.01	0.02 ± 0.00
Lungs	0.13 ± 0.02	0.65 ± 0.18 **	1.02 ± 0.13 ***	2.13 ± 0.60 **	1.68 ± 0.31 **
Heart	0.05 ± 0.00	0.64 ± 0.12 **	0.89 ± 0.22 **	0.60 ± 0.12 **	0.43 ± 0.06 ***
Liver	5.08 ± 0.52	5.76 ± 1.11	22.46 ± 5.46 **	30.59 ± 5.45 **	22.43 ± 0.67 ***
Kidneys	27.07 ± 0.74	6.49 ± 2.99 ***	7.50 ± 1.39 ***	6.46 ± 1.36 ***	4.37 ± 0.52 ***
Spleen	1.14 ± 0.32	0.93 ± 0.13	4.76 ±1.23 **	7.01 ± 1.45 **	4.66 ± 0.46 ***
Stomach	0.06 ± 0.01	0.81 ± 0.45 *	0.81 ± 0.16 **	0.97 ± 0.52 *	1.09 ± 0.52 *
Intestines	0.10 ± 0.01	1.02 ± 0.31 **	1.85 ± 0.08 ***	2.06 ± 0.26 ***	1.56 ± 0.46 **
Tumor	0.19 ± 0.03	n.d.	1.10 ± 0.60	0.57 ± 0.19 *	0.42 ± 0.10 *
Muscle (paw)	0.03 ± 0.00	0.22 ± 0.06 **	0.31 ± 0.01 ***	0.07 ± 0.03	0.08 ± 0.02 *

The significance with respect to ^{111}In-labeled Ac-TZ14011-DTPA (**11**) is indicated by the asterisks (* = P < 0.05, ** = P < 0.01, *** = P < 0.001).

Table 3

Tumor-to-muscle ratios derived from the biodistribution studies.

compound	tumor-to-muscle ratio	Relative ratio compared to compound 11
Ac-TZ14011-DTPA (**11**)	6.67 ± 0.66	1
monomer Ac-TZ14011-MSAP (**3**)	4.55 ± 0.68 *	0.68
dimer $(Ac\text{-}TZ14011)_2$-MSAP (**7**)	7.41 ± 1.87	1.11
tetramer $(Ac\text{-}TZ14011)_4$-MSAP (**10**)	5.47 ± 0.50	0.82

* $P < 0.05$ for the comparison of compound **3** with **11**.